analytical chemistry

ARTICLE

pubs.acs.org/ac

Application of Fiber-Optic Attenuated Total Reflection-FT-IR Methods for In Situ Characterization of Protein Delivery Systems in Real Time

Cathryn L. McFearin, Jagadis Sankaranarayanan, and Adah Almutairi*

School of Pharmacy and Pharmaceutical Sciences, Departments of NanoEngineering and of Materials Science and Engineering, University of California at San Diego, La Jolla, California 92093, United States

Supporting Information

ABSTRACT: A fiber-optic coupled attenuated total reflection (ATR)-FT-IR spectroscopy technique was applied to the study of two different therapeutic delivery systems, acid degradable hydrogels and nanoparticles. Real time exponential release of a model protein, human serum albumin (HSA), was observed from two different polymeric hydrogels formulated with a pH sensitive cross-linker. Spectroscopic examination of nanoparticles formulated with an acid degradable polymer shell and encapsulated HSA exhibited vibrational signatures characteristic of both particle and payload when exposed to lowered pH conditions, demonstrating the ability of this methodology to simultaneously measure phenomena arising from a system with a mixture of components. In addition, thorough characterization of these pH sensitive delivery vehicles without encapsulated protein was also accomplished in order to separate the effects of the payload during degradation. When in situ, real time detection in combination with the ability to specifically identify different components in a mixture without involved sample preparation and minimal sample disturbance is provided, the versatility and suitability of this type of experiment for research in the pharmaceutical field is demonstrated.

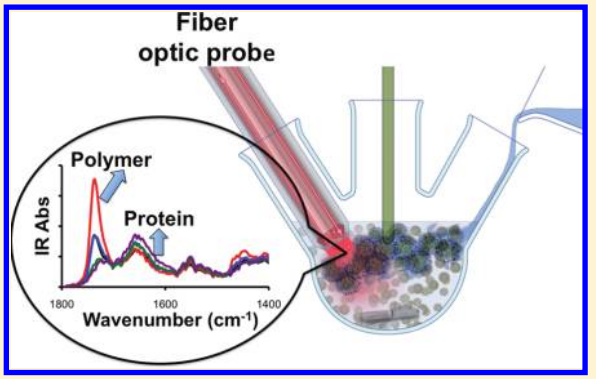

Within the pharmaceutical research field, there is a growing need for techniques that probe delivery systems comprising different biomaterials for use in drug, protein, or DNA release. Characterizing the components of these systems while obtaining release kinetics are important aspects in development with implications for the administration and efficacy of the vehicle/payload system in vivo.[1−3] Currently, many studies focusing on release rely on aliquots taken from solution at certain time points and analyzed by chromatographic and/or spectrophotometric (UV−vis, fluorescence) methods or specific analyte detection assays.[4−10] A method that could be used in situ and can detect both delivery system and payload with no involved sample preparation or purification would greatly add to the collection of methods available to researchers interested in therapeutics delivery.

Over the past decade, advances in infrared spectroscopic fiber-optic technologies, particularly those exploiting attenuated total reflection (ATR)-Fourier transform infrared (FT-IR) spectroscopy, have provided a convenient avenue for probing the complex interactions in solution.[11] These in situ fiber-optic probes have shown great success when characterizing and optimizing reaction conditions, kinetics, intermediates, and elucidating mechanisms for multicomponent mixtures.[12−14] The application of ATR-FT-IR to the study of crystal growth and nucleation shows its ability to yield valuable information from complex, multicomponent samples for pharmaceutical applications.[15,16] Despite a proven track record for acquiring real time data for a variety of different types of samples relevant to pharmaceutical research,[17,18] this methodology has not been applied to the field of therapeutic and diagnostic delivery systems often comprising buffer salt solutions, polymeric material, surfactant, and protein or other payload to be released. Here, we adapt this powerful tool to the examination of polymeric protein delivery systems. Highlighted in the current study are several applications and advantages of the in situ ATR-FT-IR method. Most notably for the protein release studies considered in this paper, this method allows detection and characterization of both the delivery vehicle and payload, often simultaneously. Additionally, this methodology can be adapted to many different reaction vessels depending on the type of system under investigation without the complex sample cell often required for constant flow or agitation in typical ATR experiments.[19] In addition, no laborious sample preparation is required such as film formation, heating, desalting, filtering, or concentration of the sample of interest, which is required for many spectrophotometric detection methods involving chromatography. The relative flexibility of the probe results in greater portability of the instrument and a smaller footprint in the laboratory.

IR spectroscopy provides a powerful alternative method for studying release phenomena from a variety of potential drug delivery systems. Detection limits are higher for IR than other methods such as RP-HPLC or other assays commonly used for

Received: March 9, 2011
Accepted: April 8, 2011
Published: April 08, 2011

quantification.[20,21] By nature, IR spectroscopy is a chemically specific technique due to its ability to probe vibrational frequencies from different functional groups, thereby providing a distinct fingerprint of the molecules under study. In addition to this specificity, vibrational peak signatures such as frequency and spectral width convey valuable information regarding the environment of the system being investigated.[22] Other benefits include information gained without using a label, as is necessary for detection by fluorescence, which can alter the native behavior of the tagged counterpart[23] and thus potentially the release behavior. Additionally, IR is a nondestructive technique and requires a relatively small amount of sample.[22] These are especially important when working with costly or scarce materials, as is often the case in drug delivery development.

Past efforts using FT-IR vibrational spectroscopy that have exploited the inherent chemical specificity of the technique to study pH responsive hydrogels did so using solid state samples prepared from dehydrated gels formed into pellets for characterization.[24] FT-IR is most often used as a general characterization method in hydrogel studies.[25] ATR-FT-IR also provided important information regarding protein adsorption to surfaces.[26−28] Han et al. used a custom built sample cell to monitor the extent of polymerization using FT-IR during hydrogel formulation for the purpose of drug delivery.[29] IR techniques have also been applied to the study of particle delivery systems. A few notable studies include work by Langer and coworkers using FT-IR to characterize protein secondary structure upon release from microspheres[30] to assess extent of denaturation during the formulation process. FT-IR spectroscopic imaging has previously been applied to the study of dissolution and release of polymer/drug formulations.[31−34] Until now, utilizing in situ FT-IR spectroscopic methods for a combination of characterization and detection of release from hydrogels had not been realized.

This paper illustrates the power of the in situ ATR-FT-IR fiber-optic probe technology by examining two different systems important to the drug delivery field, hydrogels and nanoparticles, with an encapsulated model protein human serum albumin (HSA). These protein delivery systems are characterized with the high level of chemical specificity inherent to IR spectroscopy. Additionally, we detect, in real time, the release of encapsulated model protein upon applied external stimulus with no specialized sample preparation necessary for the experiment. Hydrogels sensitive to pH environment,[35] formed with an acid degradable cross-linker,[36] facilitate triggered release of the protein when in contact with a low pH aqueous environment, as is found in tumors and diseased tissue.[37,38] Polymers that are pH sensitive,[39,40] previously synthesized and characterized in our laboratory,[41] make up the particle shell and encapsulate the protein. When exposed to acidic conditions, the polymer coating breaks apart releasing the payload.

We monitor both the degradation of the polymeric delivery materials as well as the release of encapsulated protein by following the IR absorbance signals and the specific vibrational frequencies of those bands attributed to these different components. These spectral parameters provide a qualitative picture of the systems' degradation and release mechanisms, which provides vital information necessary for biomaterial development.

EXPERIMENTAL SECTION

Synthesis of pH Sensitive Materials. The acid degradable cross-linker was prepared according to literature procedures.[42]

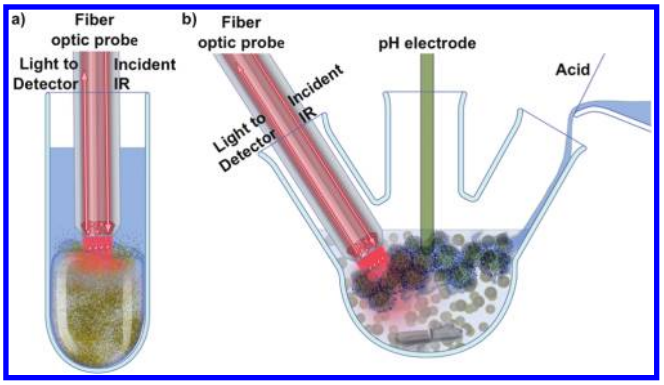

Figure 1. Schematic of the in situ ATR-FT-IR sample vessels: (a) hydrogel lies in the bottom of a vial with the acidic buffer and probe above; (b) three-neck round-bottom flask allows access to the nanoparticle suspension for the probe, pH electrode, and acid.

The poly β-aminoester ketal polymer (referred to here as random copolymer) has been synthesized and characterized previously in our laboratory.[41] This synthesis and the formation of the hydrogels and particles are described in the Supporting Information section.

In Situ ATR Setup. The IR measurements were obtained using a ReactIR 45 m spectrophotometer (Mettler Toledo) equipped with a liquid nitrogen-cooled MCT detector and the 9.5 mm AgX DiComp probe housing a diamond ATR crystal. The spectrophotometer was continuously purged with dry nitrogen during the measurements. The IR spectra were obtained in the 700−2400 cm^{-1} range. Spectra were taken with an average of 256 scans per sample and a spectral resolution of 4 cm^{-1}. Baseline correction, ambient and solvent background subtraction, and peak height to single baseline calculations were performed for all spectra within the instrument software (iC IR). The baseline was a single point offset; however, using alternative correction functions did not result in different spectral trends. Figure 1 shows a schematic of the different sample setups used in the hydrogel and particle experiments. Figure 1a,b depicts the hydrogel and nanoparticle sample configurations, respectively. More in depth details on the setup, measurements, and spectral analysis can be found in the Supporting Information section.

RESULTS AND DISCUSSION

There are two primary absorptions from proteins within this frequency region of interest, the amide I and amide II vibrational bands (Supporting Information, SI Figure 1 illustrates the chemical structures of the peptide backbone and a representative IR spectrum of HSA). The amide I vibrational band (~1650 cm^{-1}) comprises mainly the C═O stretching vibrations of the peptide groups. The amide II (~1550 cm^{-1}) vibration results from the NH in-plane bend and partially from the CN stretching vibrations.[43] The amide I band has the most single component nature, meaning that it mostly comes from the C═O stretch unlike the amide II which has more contributions from other vibrational modes,[43] so it is most commonly used for characterization of proteins by IR spectroscopy. Therefore, the remainder of the protein analysis presented here will focus on the amide I band rather than amide II.

Hydrogels. Figures 2a and 3a show the IR spectra of the empty (no protein encapsulated) polyacrylamide and polyethylene glycol acrylate (PEGA) hydrogels, respectively. Shown in both

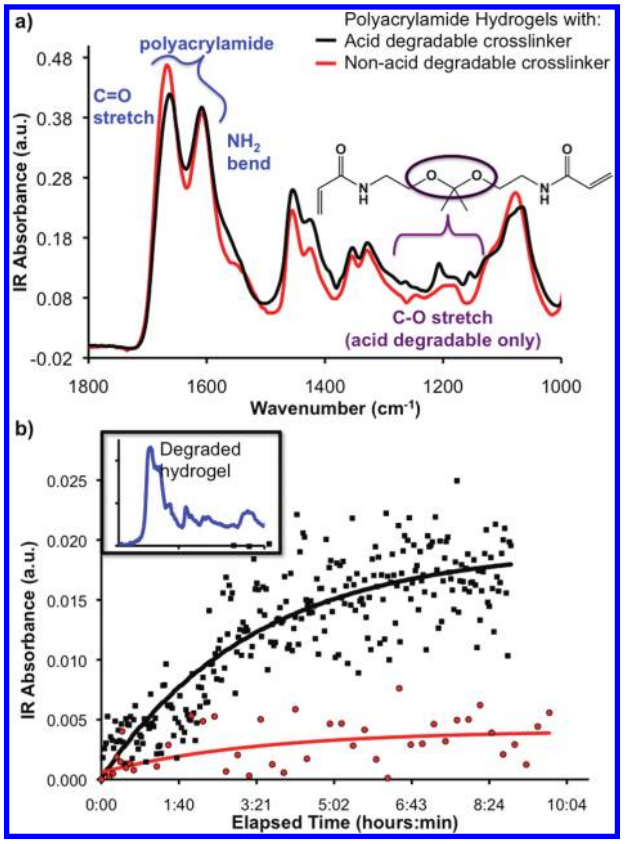

Figure 2. (a) IR spectra and major vibrational assignments of polyacrylamide hydrogels formulated with the acid degradable cross-linker (black trace) and a non-acid degradable cross-linker bisacrylamide (red trace) with no encapsulated protein and the chemical structure of the acid degradable cross-linker. (b) Peak height to a single baseline IR absorbance of the amide I C═O stretch of released HSA at pH 5 over time from hydrogels formulated with the acid degradable cross-linker (black squares) and a non-acid degradable cross-linker bisacrylamide (red circles). Markers are data points, and the solid lines are fits to the data. Inset: IR spectrum after hydrogel degradation showing the polyacrylamide vibrational bands in addition to the released protein.

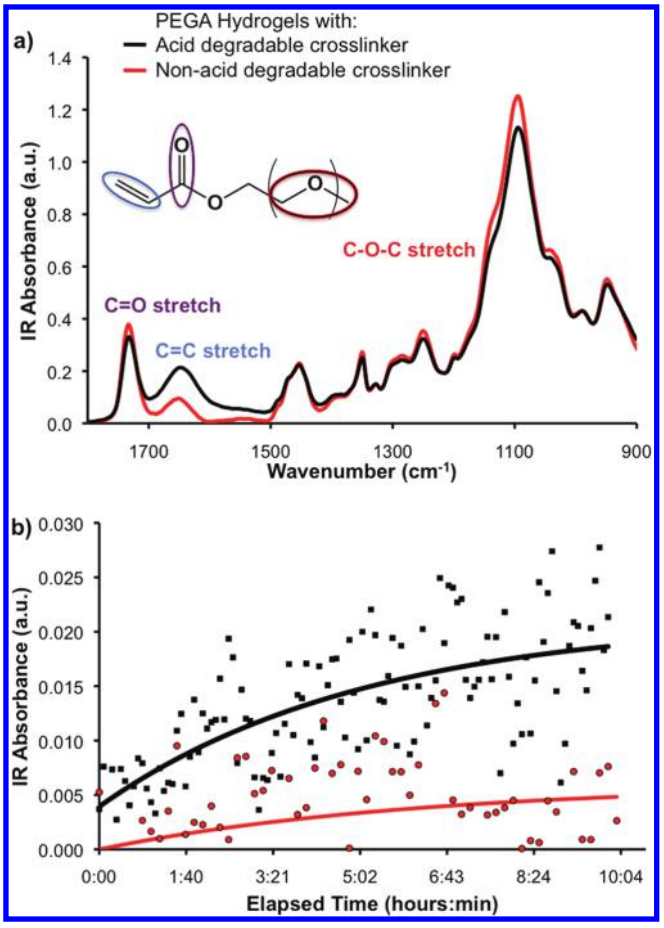

Figure 3. (a) IR spectra and major vibrational assignments of PEGA hydrogels formulated with the acid degradable cross-linker (black trace) and a non-acid degradable cross-linker bisacrylamide (red trace) with no encapsulated protein and the chemical structure of PEGA. (b) Peak height to a single baseline IR absorbance of the amide I C═O stretch of released HSA at pH 5 over time from hydrogels formulated with the acid degradable cross-linker (black squares) and a non-acid degradable cross-linker bisacrylamide (red circles). Markers are data points, and the solid lines are fits to the data.

figures are spectra of hydrogels formulated with the acid degradable cross-linker (black traces) as well as a non-acid degradable cross-linker bisacrylamide (red traces). In Figure 2a, the two most prominent vibrational bands appear at 1665 and 1610 cm^{-1} indicative of the C═O stretch and NH_2 bending motions, respectively, from polyacrylamide.[44] Below 1500 cm^{-1}, there are also relatively strong spectral signatures for CN and CH modes present in the polymers of both hydrogel formulations. The pH sensitive cross-linker spectral signatures emerge at ∼1200−1150 cm^{-1} due to the C−O stretch from the ketal groups, which are not present in the hydrogels cross-linked with bisacrylamide. In Figure 3a, the PEGA hydrogels exhibit a strong absorbance at 1090 cm^{-1} from the C−O−C stretching vibrations of the polymer with weaker contributions at the higher energy portion of the spectrum attributed to the C═O (∼1730 cm^{-1}) and C═C (∼1650 cm^{-1}) stretches from the unreacted monomer.[45] This ability to unambiguously detect the degree of polymerization is very important and can be crucial for systems where unreacted monomer can be toxic.[46] These spectra provide a detailed characterization of the hydrogels, in particular the subtle differences between the two cross-linked formulations, which is necessary in order to distinguish any release spectral signatures from those due to polymer degradation.

The protein release profiles over time of both the polyacrylamide and PEGA hydrogels formulated with both an acid degradable cross-linker and with bisacrylamide are shown in Figures 2b and 3b. The data depict the IR absorbance at 1650 cm^{-1} calculated as the height of the spectral peak to a single point baseline as a function of time. The measured absorbances tracked in these plots are attributed to the amide I (C═O stretch) group from the protein. In all the traces shown, the *x*-axis time value starts when the acidified buffer solution was added to the vial containing the hydrogel. The data have been normalized to a starting absorbance value of zero by subtracting each measured data point from the initial, time = 0 h, absorbance value. For each hydrogel system, there was spectral evidence of protein detected at time = 0 h due to protein on the hydrogel surface that is immediately released into solution when the buffer is added.

Figures 2 and 3 show that over time there is an increase in the amide I absorbance peak height for both the acid degradable

dx.doi.org/10.1021/ac200591a |*Anal. Chem.* 2011, 83, 3943–3949

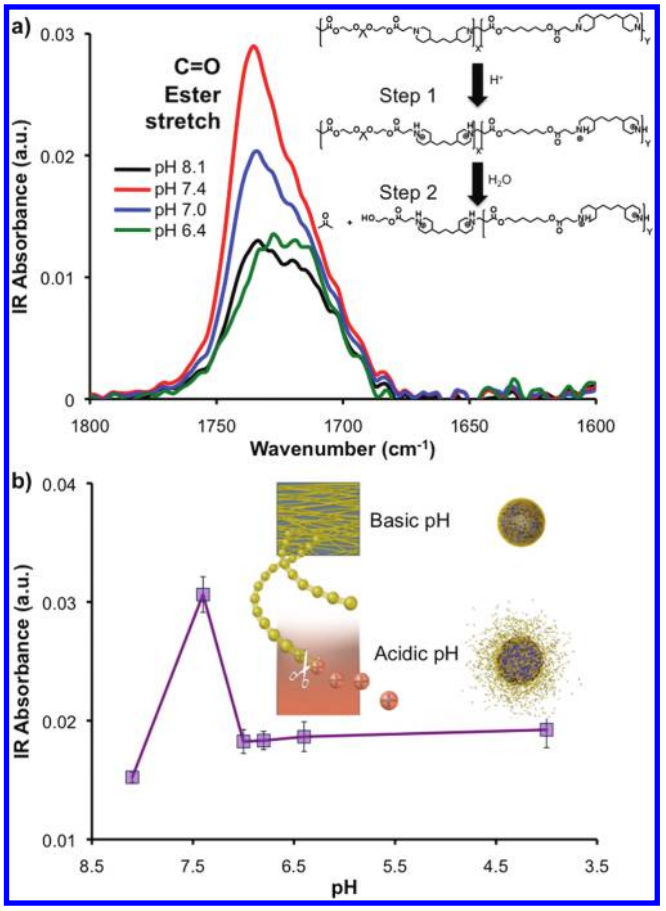

Figure 4. (a) IR spectra of empty particles formulated from the random copolymer at different pH values. Mechanism showing exposure to mildly acidic conditions facilitates Step 1, protonation of amines, allowing Step 2, hydration followed by fragmentation of polymer. (b) Ester peak heights as a function of pH. Cartoon of random copolymer particle degradation.

cross-linked hydrogels (black squares) and non-acid degradable/bisacrylamide cross-linked hydrogels (red circles) albeit to differing degrees. This holds for both the polyacrylamide and the PEGA hydrogels. The IR absorbance of the amide II band (NH bend, ~1550 cm^{-1}) also increases (not shown), but the trend is far less pronounced.

Because the sample configuration is such that any IR signal must arise from components in the aqueous buffer solution, the increase in absorbance of the amide I bands depicted in Figures 2b and 3b provide evidence of the real time release of HSA from the hydrogels. Importantly, these plots convey information regarding the kinetic release profiles specific to the composition of the hydrogel. First, the hydrogels formulated with the acid degradable cross-linker exhibit exponential increases in protein absorbance signal consistent with the ketal hydrolysis kinetics[36,47] that govern the degradation of the hydrogel and in turn the release of the protein. Once the hydrogel is in contact with the acidified buffer solution (time = 0 h), the IR absorbance of the amide I peak begins to increase over a period of ~3 h. The rate of increase then slows and eventually levels off with little to no change in absorbance observed after 10 h. Interestingly, the overall behavior and even the time frame are similar for both the polyacrylamide and the PEGA hydrogels.

To ensure that these release kinetics reflected a triggered release response upon exposure to low pH and not simply diffusion of the protein into the solution, hydrogels were formulated with a non-pH sensitive cross-linker (at the same molar ratio), bisacrylamide. In contrast to the exponential increase of IR absorbance over several hours, observed for the acid degradable systems, the bisacrylamide cross-linked hydrogels show an exponential increase over ~1.5 h after which the absorbance levels off for both polymeric systems. The small initial increase in amide I signal is likely due to diffusion of the protein from the surface of the hydrogel over the short time. The amide I IR absorbance values at the end of the time frame of the experiments are lower for both polymeric hydrogels formulated with the bisacrylamide cross-linker compared to those formed with the acid degradable cross-linker, indicating that less protein was released during this time.

The ability to distinguish between these types of release kinetics is critical for a thorough in vitro characterization of any delivery system behavior and is readily obtained with the ATR probe technology utilized here. To verify these results, HSA release was also monitored by UV absorption in a separate set of experiments using hydrogels prepared identically to those presented in Figures 2 and 3. These results found in the Supporting Information (SI Figure 2) corroborate the release kinetics determined from IR. They also illustrate a key advantage of the in situ ATR-IR probe experiments over those from SI Figure 2 (Supporting Information) or other types of similar experiments, although this is not apparent from merely examining the plots. The IR probe technology does not require taking aliquots at certain time intervals for analysis. These labor and time intensive experiments (release profiles took the better part of a day each) are avoided by simply placing the ATR probe in the solution under investigation and beginning the spectral acquisition, thereby saving a great deal of time and effort, which is invaluable to any researcher.

Another key advantage of this type of in situ ATR-IR spectroscopy is the ability to differentiate between different chemical components within a mixture. With the current setup, the ATR probe facilitates this by sampling the heterogeneous solution composition during each spectrum. The inset (blue trace) shown in Figure 2b illustrates this point. It shows a spectrum of the pH 5 buffer solution obtained after exposure to the polyacrylamide hydrogel with the acid degradable cross-linker for 10 h. Unlike the spectrum shown in SI Figure 1 (Supporting Information), there are more peaks present than just the amide I and II vibrational bands from the released protein, which are due to the degradation products of the polyacrylamide hydrogel. In particular, the C═O stretch of the acrylamide grows in on the high frequency side of the amide I peak as seen in the empty gel spectrum in Figure 2a. Although there is overlap between the two peaks, the resolution is high enough to readily distinguish between the different components of the protein delivery system obtained simultaneously without any additional experimental or sample manipulation, unlike other techniques commonly employed for payload release studies.

Nanoparticles. Another important mode of protein delivery is through encapsulation in nanoparticles with degradable polymer shells, which release their payload through a variety of different mechanisms depending on the polymer's chemical makeup. An acid sensitive poly β-aminoester ketal polymer (referred to here as random copolymer), previously synthesized and characterized for this purpose by our laboratory,[41] was chosen to illustrate the

ability of the ATR probe to characterize this method of protein delivery. The random copolymer shell has one predominant vibrational mode in the spectral window of interest with a central frequency at 1735 cm^{-1} (shown in SI Figure 3, Supporting Information). This is attributed to the C═O stretch from the ester groups on the polymer backbone, which are circled on the chemical structure of the polymer shown in SI Figure 3, Supporting Information.

IR vibrational spectra of the particle suspensions formulated from the random copolymer without HSA at different pH values are shown in Figure 4a. These spectra focus solely on the ester peak trends and reflect what is occurring within the particles' polymer shell as the pH of the suspension undergoes a shift from basic to acidic leading to degradation of the particle shell.

Figure 4b shows the absorbance peak height of the ester vibrational mode at different pH values. During the initial spectral acquisition of the particle solution at basic pH, the polymer shell is insoluble in aqueous conditions and the solution is a turbid particle suspension (Figure 4a, black trace). With a slight decrease in pH to 7.4 (Figure 4a, red trace) of the solution, there is an increase in absorbance of the ester peak. Upon further lowering the pH to neutral (Figure 4a, blue trace), the peak then decreases. The suspension begins to visibly clear. At slightly acidic pH conditions, the peak height of the green trace in Figure 4a is approximately the same height as in the initial basic solution and the solution is no longer turbid. Further decreasing the solution pH does not result in any difference in spectral appearance or peak height as shown in Figure 4b. In addition to the ester peak IR absorbance changes as the pH is lowered, there is also a shift in frequency observed in Figure 4a. The center peak frequency of the C═O ester stretch at basic and neutral pH is 1736 cm^{-1}. When the particle suspension pH is made slightly acidic (6.4 and lower), the ester C═O mode has a final vibrational frequency of 1715 cm^{-1}.

Further examination of these trends reveals insight into the behavior of the polymer particle shell as the pH of the suspension is lowered. The mechanism in Figure 4a shows how the random copolymer degrades, leading to fragmentation of the particles depicted by the cartoon in Figure 4b. Previous characterization of the polymer[41] showed decreasing the pH results in protonation of the amines along the polymer backbone, rendering the polymer more hydrophilic. Once the polymer becomes more hydrophilic, it also has a higher aqueous solubility, allowing increased uptake of water. Comparing the vibrational frequencies of the C═O stretching mode in both solid form (SI Figure 3, Supporting Information) and suspended as the particle shell in slightly basic or neutral aqueous conditions (Figure 4a), it appears at the same vibrational energy (~1735 cm^{-1}). This indicates that the environment within the particle shell is similar to a thin film of polymer. As the polymer shell of the particle "sees" a more aqueous environment upon further lowering the pH of the suspension, there is a larger degree of dipole interaction capabilities between the ester C═O groups on the polymer with their surroundings. In this case, that could be either water molecules in the solvent or nearby positively charged amine groups. A higher degree of intermolecular interaction of these C═O stretching modes results in a decrease in vibrational frequency, indicative of a more highly coordinated or bonded environment,[22] as is shown in Figure 4a. Hydration of the polymer shell is then followed by acid catalyzed hydrolysis of the ketal groups along the polymeric backbone. The degradation products of the polymer in acidic conditions were verified by NMR.[41]

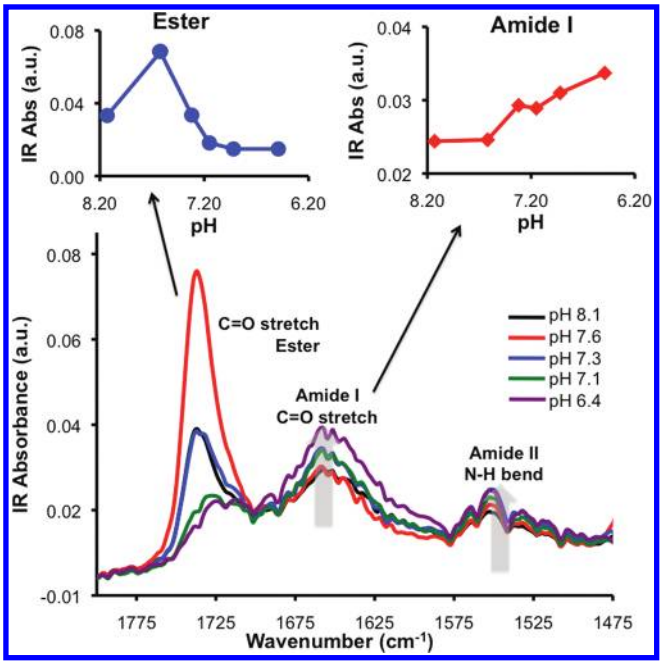

Figure 5. Top: Peak absorption versus pH for the ester and amide I vibrations. Bottom: Random copolymer IR spectra at different solution pH values during particle degradation. Gray arrows indicate direction of amide bond absorbance trend with lowered pH.

To verify that the trends in Figure 4a,b are specific to the random copolymer mechanism in Figure 4a, empty particles were also formulated with a non-acid degradable polymer poly(lactic-*co*-glycolic acid) (PLGA). Spectra of these particles under the same pH conditions as in the random copolymer case (SI Figure 4a, Supporting Information) show two vibrational modes within the same spectral region. One is the C═O ester stretch (1760 cm^{-1}) from the polymer, and the other is a C═O stretch from the carboxylic acid group (1720 cm^{-1}). Unlike the ester stretch mode seen in Figure 4 for the random copolymer particles, there are no frequency shifts for either C═O mode present as the pH of the PLGA particle solution goes from basic to acidic. The peak height of the ester stretch as a function of pH (SI Figure 4b, Supporting Information) exhibits little change in absorbance as the suspension drops below pH 6. Together, this shows that the spectral trends depicted in Figure 4 for the particles composed of the random copolymer pertain to the acid degradable characteristics unique to its chemical makeup. The degradation at mildly acidic conditions is captured by the vibrational spectroscopic trends shown here without any purification or manipulation of the particle suspensions, demonstrating the suitability of this method for characterization of polymeric particle systems.

Figure 5 shows IR spectra of particles formulated from the random copolymer encapsulating HSA at different pH values. The three vibrational bands of interest present in these spectra are the C═O ester stretch from the polymer backbone and the amide I and II vibrations from HSA. The peak absorbance height trends for the ester (blue trace) and amide I (red trace) modes are plotted versus pH as well in Figure 5. Starting with the high energy portion of the spectra, the ester stretch mode behavior exhibits an initial increase in absorbance followed by a decrease that levels off with sequential additions of acid. The stretching frequency of the C═O mode also undergoes a shift to lower energy upon lowering the pH of the particle suspension. These

data are very similar to what was shown for the empty particles in Figure 4, indicating that the presence of the protein does not greatly influence the polymer shell degradation. While this may not hold for all payloads envisioned for delivery using this type of particle, it is promising that a potential therapeutic with such a relatively large size as a serum albumin protein does not interfere with the acid degradable properties of the particle which are vital for use in delivery to areas exhibiting slightly acidic conditions as are found in tumors and diseased tissue. This finding provides yet another example of the utility of the current IR method for therapeutic delivery research where in situ, simultaneous examination of all components of a system gives a much more complete picture than simply examining the payload alone.

In addition to the ester peak trends, Figure 5 also displays an increase in absorbance for the protein vibrational amide I signature as the pH of the solution is lowered. It is important to note here that the particle suspension is only stable in slightly basic conditions, so in order to monitor degradation, the pH must be lowered in a fashion that involves dynamic changes in both acid and protein concentration, thereby complicating the spectral interpretation. In the hydrogel experimental setup from the previous section, the pH could be kept constant and changes in protein concentration were measured in solution that could be directly attributed to HSA released from the gel. Comparing the magnitude of change in IR absorbance peak height versus pH for the acid degradable hydrogels (Figures 2b and 3b) to that of the nanoparticles (Figure 5), we see that both systems show a similar degree of increase in amide I protein absorbance. These similarities are likely due to the use of a similar acid degradable chemical structure used for the cross-linker and the polymer shell for both the hydrogel and particle systems, respectively. However, we cannot solely attribute these increases to release from the particles because spectra acquired of the protein in solution (no polymer) with added acid also showed slight increases in absorbance. The spectra reveal a vibrational response of the protein from a combination of factors as the polymer shell degrades upon making the particle suspension acidic, including release from the inner aqueous layer of the particle and exposure to slightly acidic conditions as the water uptake of the particle increases. The lack of a frequency shift for either amide vibrations throughout the pH series signifies retention of a similar aqueous solvation environment surrounding the protein throughout the particle degradation process. The spectra shown in Figure 5 exemplify the ability of the current spectroscopic method to concurrently analyze both the particle and the payload during a given experiment.

CONCLUSIONS

As interest in protein delivery continues to increase and new delivery materials are developed,[48,49] methods for studying these materials must be established that provide adaptability and ease of data acquisition. To our knowledge, this is the first demonstration of in situ vibrational infrared spectroscopy for the real time monitoring of protein release. We have shown that the combination of ATR-IR spectroscopy with a fiber-optic probe allows real time, in situ examination of both pH responsive hydrogels and nanoparticles that undergo degradation when exposed to mildly acidic conditions. When chemically specific vibrational frequencies are examined, these two important therapeutic delivery systems are characterized with and without an encapsulated model protein, human serum albumin. Both materials show different behavior when exposed to acid in comparison to their non-acid degradable counterparts commensurate with their chemical degradation kinetics. The real time pH stimulated protein release from two different widely used hydrogels was directly probed without any modification or complex sample manipulation. The process of particle degradation was followed with and without protein, giving further insight into the complex environment present in polymeric nanomaterials.

The methodology presented here can be applied to research involving protein diffusion through hydrogels such as characterization of the presentation of growth factors.[50] IR spectroscopy also allows for further characterization of the released protein by probing secondary structure to determine integrity after formulation.[30,51,52] Future endeavors in the realm of pharmaceutical delivery include the ability to probe different types of systems such as drug release profiles. In addition, the nondestructive nature of the technique makes it ideal for the extension of studies to the in vivo realm.[53,54]

ASSOCIATED CONTENT

Supporting Information. Materials, synthesis, and formulation of acid sensitive particles and hydrogels. In situ ATR setup, spectral acquisition, and analysis. Vibrational spectra of HSA and the acid degradable poly β-amino ester (random copolymer). Release of HSA detected by absorbance and spectra of PLGA particles. This material is available free of charge via the Internet at http://pubs.acs.org.

AUTHOR INFORMATION

Corresponding Author
*E-mail: aalmutairi@ucsd.edu.

ACKNOWLEDGMENT

The authors acknowledge the PhRMA Foundation and the NIH New Innovator Award (DP 2OD006499) for funding this research.

REFERENCES

(1) Davis, M. E.; Chen, Z.; Shin, D. M. *Nat. Rev. Drug Discovery* **2008**, *7*, 771–782.
(2) Wagner, V.; Dullaart, A.; Bock, A. K.; Zweck, A. *Nat. Biotechnol.* **2006**, *24*, 1211–1217.
(3) Zhang, L.; Gu, F. X.; Chan, J. M.; Wang, A. Z.; Langer, R. S.; Farokhzad, O. C. *Clin. Pharmacol. Ther.* **2008**, *83*, 761–769.
(4) Argentiere, S.; Blasi, L.; Ciccarella, G.; Barbarella, G.; Cingolani, R.; Gigli, G. *J. Appl. Polym. Sci.* **2010**, *116*, 2808–2815.
(5) Corrigan, O. I.; Li, X. *Eur. J. Pharm. Sci.* **2009**, *37*, 477–485.
(6) Mora, L.; Chumbimuni-Torres, K. Y.; Clawson, C.; Hernandez, L.; Zhang, L. F.; Wang, J. *J. Controlled Release* **2009**, *140*, 69–73.
(7) Wang, X.; Hu, X.; Daley, A.; Rabotyagova, O.; Cebe, P.; Kaplan, D. L. *J. Controlled Release* **2007**, *121*, 190–199.
(8) Weiner, A. A.; Bock, E. A.; Gipson, M. E.; Shastri, V. P. *Biomaterials* **2008**, *29*, 2400–2407.
(9) Weinstain, R.; Segal, E.; Satchi-Fainaro, R.; Shabat, D. *Chem. Commun.* **2010**, *46*, 553–555.
(10) Yang, C. M.; Plackett, D.; Needham, D.; Burt, H. M. *Pharm. Res.* **2009**, *26*, 1644–1656.
(11) Harrington, J. A., Ed. *Infrared fibers and their applications*; SPIE Optical Engineering Press: Bellingham, WA, 2004.
(12) Hua, H.; Dube, M. A. *Polym. React. Eng.* **2002**, *10*, 21–40.
(13) Poljansek, I.; Krajnc, M. *Acta Chim. Slov.* **2005**, *52*, 238–244.

(14) Poljansek, I.; Likozar, B.; Krajnc, M. *J. Appl. Polym. Sci.* **2007**, *106*, 878–888.
(15) Togkalidou, T.; Fujiwara, M.; Patel, S.; Braatz, R. D. *J. Cryst. Growth* **2001**, *231*, 534–543.
(16) Togkalidou, T.; Tung, H. H.; Sun, Y. K.; Andrews, A.; Braatz, R. D. *Org. Process Res. Dev.* **2002**, *6*, 317–322.
(17) Conlon, D.; McWilliams, C. J.; Reamer, R.; Izzo, B.; Collins, P.; Xu, F. *Process Chemistry in the Pharmaceutical Industry*, 2nd ed.; CRC Press: Boca Raton, FL, 2008.
(18) Conlon, D.; Izzo, B.; Collins, P. *Process Chemistry in the Pharmaceutical Industry*, 2nd ed.; CRC Press: Boca Raton, FL, 2008.
(19) Vigano, C.; Ruyssehaert, J. M.; Goormaghtigh, E. *Talanta* **2005**, *65*, 1132–1142.
(20) Umrethia, M.; Kett, V.; Andrew, G.; Malcolm, K.; Woolfson, D. *J. Pharm. Pharmacol.* **2009**, *61*, A28–A28.
(21) Umrethia, M.; Kett, V. L.; Andrews, G. P.; Malcolm, R. K.; Woolfson, A. D. *J. Pharm. Biomed. Anal.* **2010**, *51*, 1175–1179.
(22) Stuart, B. H. *Infrared Spectroscopy: Fundamentals and Applications*, 1st ed.; John Wiley & Sons, Ltd: Hoboken, NJ, 2004.
(23) Teske, C. A.; Schroeder, M.; Simon, R.; Hubbuch, J. r. *J. Phys. Chem. B* **2005**, *109*, 13811–13817.
(24) Wang, L.; Liu, M.; Gao, C.; Ma, L.; Cui, D. *React. Funct. Polym.* **2010**, *70*, 159–167.
(25) Gai, L.; Wu, D. *Appl. Biochem. Biotechnol.* **2009**, *158*, 747–760.
(26) Bummer, P. M. *Int. J. Pharm.* **1996**, *132*, 143–151.
(27) Chittur, K. K. *Biomaterials* **1998**, *19*, 357–369.
(28) Lenk, T. J.; Ratner, B. D.; Gendreau, R. M.; Chittur, K. K. *J. Biomed. Mater. Res.* **1989**, *23*, 549–569.
(29) Han, J.; He, Y.; Xiao, M.; Ma, G. P.; Nie, J. *Polym. Adv. Technol.* **2009**, *20*, 607–612.
(30) Fu, K.; Griebenow, K.; Hsieh, L.; Klibanov, A. M.; Langer, R. *J. Controlled Release* **1999**, *58*, 357–366.
(31) Bobiak, J. P.; Koenig, J. L. *J. Controlled Release* **2005**, *106*, 329–338.
(32) Chan, K. L. A.; Kazarian, S. G. *Mol. Pharmaceutics* **2004**, *1*, 331–335.
(33) Coutts-Lendon, C. A.; Wright, N. A.; Mieso, E. V.; Koenig, J. L. *J. Controlled Release* **2003**, *93*, 223–248.
(34) Kazarian, S. G.; Chan, K. L. A. *Appl. Spectrosc.* **2010**, *64*, 135A–152A.
(35) You, J.-O.; Auguste, D. T. *Langmuir* **2010**, *26*, 4607–4612.
(36) Murthy, N.; Thng, Y. X.; Schuck, S.; Xu, M. C.; Frechet, J. M. J. *J. Am. Chem. Soc.* **2002**, *124*, 12398–12399.
(37) Tannock, I. F.; Rotin, D. *Cancer Res.* **1989**, *49*, 4373–4384.
(38) Vaupel, P.; Kallinowski, F.; Okunieff, P. *Cancer Res.* **1989**, *49*, 6449–6465.
(39) Guo, X.; Szoka, F. C. *Acc. Chem. Res.* **2003**, *36*, 335–341.
(40) Huang, Z.; Guo, X.; Li, W.; MacKay, J. A.; Szoka, F. C. *J. Am. Chem. Soc.* **2005**, *128*, 60–61.
(41) Sankaranarayanan, J.; Mahmoud, E. A.; Kim, G.; Morachis, J. M.; Almutairi, A. *ACS Nano* **2010**, *4*, 5930–5936.
(42) Jain, R.; Standley, S. M.; Frechet, J. M. J. *Macromolecules* **2007**, *40*, 452–457.
(43) Barth, A.; Zscherp, C. *Q. Rev. Biophys.* **2002**, *35*, 369–430.
(44) Murugan, R.; Mohan, S.; Bigotto, A. *J. Korean Phys. Soc.* **1998**, *32*, 505–512.
(45) Zanini, S.; Riccardi, C.; Grimoldi, E.; Colombo, C.; Villa, A. M.; Natalello, A.; Gatti-Lafranconi, P.; Lotti, M.; Doglia, S. M. *J. Colloid Interface Sci.* **2010**, *341*, 53–58.
(46) Smith, E. A.; Oehme, F. W. *Rev. Environ. Health* **1991**, *9*, 215–228.
(47) Fife, T. H.; Hagopian, L. *J. Org. Chem.* **1966**, *31*, 1772–1775.
(48) Benoit, D. S. W.; Henry, S. M.; Shubin, A. D.; Hoffman, A. S.; Stayton, P. S. *Mol. Pharmaceutics* **2010**, *7*, 442–455.
(49) Garbern, J. C.; Hoffman, A. S.; Stayton, P. S. *Biomacromolecules* **2010**, *11*, 1833–1839.
(50) Marklein, R. A.; Burdick, J. A. *Adv. Mater.* **2010**, *22*, 175–189.
(51) Bramanti, E.; Benedetti, E. *Biopolymers* **1996**, *38*, 639–653.
(52) Vonhoff, S.; Condliffe, J.; Schiffter, H. *J. Pharm. Biomed. Anal.* **2010**, *51*, 39–45.
(53) Downes, A.; Mouras, R.; Elfick, A. *J. Biomed. Biotechnol.* **2010**, *2010*, Article ID 101864.
(54) Chan, J. W.; Lieu, D. K. *J. Biophotonics* **2009**, *2*, 656–668.